INTERNATIONAL JOURNAL FOR NUMERICAL METHODS IN ENGINEERING
Int. J. Numer. Meth. Engng. **44**, 1481–1504 (1999)

A MIXED-ENHANCED FINITE-ELEMENT FOR THE ANALYSIS OF LAMINATED COMPOSITE PLATES

FERDINANDO AURICCHIO[1] AND ELIO SACCO[2,*]

[1] *Dipartimento di Ingegneria Civile, Università di Roma "Tor Vergata", Italy*
[2] *Dipartimento di Ingegneria Industriale, Università di Cassino, Italy*

SUMMARY

This paper presents a new 4-node finite-element for the analysis of laminated composite plates. The element is based on a first-order shear deformation theory and is obtained through a mixed-enhanced approach. In fact, the adopted variational formulation includes as variables the transverse shear as well as enhanced incompatible modes introduced to improve the in-plane deformation. The problem is then discretized using bubble functions for the rotational degrees of freedom and functions linking the transverse displacement to the rotations. The proposed element is locking free, it does not have zero energy modes and provides accurate in-plane/out-of-plane deformations. Furthermore, a procedure for the computation of the through-the-thickness shear stresses is discussed, together with an iterative algorithm for the evaluation of the shear correction factors. Several applications are investigated to assess the features and the performances of the proposed element. Results are compared with analytical solutions and with other finite-element solutions. Copyright © 1999 John Wiley & Sons, Ltd.

KEY WORDS: composite laminates; finite elements; mixed-enhanced formulation; shear stress recovery; shear correction factors

1. INTRODUCTION

Composite materials find great interest in a variety of complex structures, such as those typically adopted in space, automobile and civil applications. The design of these structures clearly requires numerical tools able to perform accurate stress analyses. As a matter of fact, nowadays many commercial finite-element codes contain laminated composite plate and shell elements.

However, the proper modelling of laminated plates is a non-trivial task and it can be still considered as an open research problem mainly as a consequence of their complex behaviour. In fact, composite laminates have in general an anisotropic response, present significant shear deformation in the thickness and extension-bending coupling. Furthermore, the determination of accurate values for the interlaminar normal and shear stresses is of crucial importance, since they are responsible for the activation and the development of delamination mechanisms. A satisfactory laminate theory and a corresponding reliable finite-element have to capture all these effects.

* Correspondence to: Elio Sacco, Dipartimento di Ingegneria Industriale, Universita di Cassino, Via di Biasio 43, Cassino 03043, Italy. E-mail: sacco@ing.unicas.it

Contract/grant sponsor: CNR
Contract/grant sponsor: MURST
Contract/grant sponsor: ASI

CCC 0029–5981/99/101481–24$17.50

Received 2 April 1997
Revised 23 March 1998

Several laminate theories have been proposed in the literature. The first and simplest one is the classical laminate theory (CLT);[1, 2] based on the Kirchhoff–Love assumptions, the CLT neglects the shear deformation and, as a consequence, it can lead to inaccurate results.

The extension of the Reissner[3] and Mindlin[4] models to the case of laminated anisotropic plates is of great interest for the possibility of taking into account shear deformation effects in a simple way.[5, 6] Indicated in the following as First-order Shear-Deformation Theory (FSDT), this approach gives satisfactory results for a wide class of structural problems, even for moderately thick laminates. In particular, accurate results are obtained if proper values for the shear correction factors are adopted.

However, the determination of the shear factors is non-trivial, since they depend on the lamination sequence and on the deformation state. Hence, the value 5/6 is often used, which is exact only for homogeneous plates.

Closed-form expressions for the shear factors can be obtained only for very simple cases. As an example, Whitney[7] solved the problem for cross-ply laminates under cylindrical bending and, more recently, the same approach has been reviewed in References 8 and 9. These works highlight how the shear factors can assume values which are quite different from 5/6.

A numerical procedure for improving the FSDT results has been proposed by Noor and co-workers.[10–12] Assuming initial values for the shear factors, the FSDT is used to predict the laminate response; based on this solution, new values for the shear factors are computed and used again with the FSDT; finally, through-the-thickness displacements and stresses are determined via integration. So far, the procedure has been applied only to problem for which analytical solutions are available, while no extensions to the finite-element framework have been presented.

Recently, refinements of the FSDT have also been proposed. For example, Pai[13] considered additive shear warping functions and developed a technique for an *a priori* estimate of shear factors. Yunquin Qi *et al.*[14] assumed that transverse shear strain varies in the thickness of a cross-ply laminate in cylindrical bending with the same law of the shear stress obtained by the integration of the equilibrium equations.

Higher-order laminate theories have also been developed to overcome the limitations of the FSDT. Two different approaches can be distinguished: single-layer and multi-layer formulations. The first class of theories increases the order of the terms considered for the displacement representation in the thickness coordinates, e.g. References 15 and 16. The second class of theories assumes a representation formula for the displacement field in each layer, e.g. References 17–19.

From a computational point of view, several finite elements for laminated plates have been proposed in the literature. For instance, a continuum 8-node elements for a second-order composite laminate theory has been proposed in References 20 and 21. Hybrid and partial hybrid stress elements have been developed for FSDT, e.g. References 22 and 23, respectively. Recently, Yong *et al.*[24] presented a partial hybrid stress element for the higher-order shear deformation theory of Lo *et al.*[15] A 3-D finite element for laminated composites is developed in Reference 25 for layerwise theory.

In conclusion, a review of the literature shows how the FSDT gives the best compromise between prediction ability and computational costs for a wide class of problems. This is especially true if proper shear factors are used during the analysis. Furthermore, the 4-node elements are often preferred with respect to 8- or 9-node ones since they allow simplest discretization procedures, as well as easier extensions to finite deformation regimes. On the other hand, 4-node displacement-based elements adopt simple interpolation functions, which do not allow a satisfactory recovery of the through-the-thickness shear stresses. According to these considerations, this paper presents a

new 4-node FSDT finite element for laminated composite plate. The element is based on a mixed-enhanced formulation and uses enhanced incompatible modes to improve the in-plane deformation, bubble functions for the rotational degrees of freedom and functions linking the transverse displacement to the rotations. The element is locking free, it does not have zero energy modes and is able to provide accurate in-plane/out-of-plane deformations. Moreover, an important feature consists in the unusual possibility for a 4-node element to recover accurate through-the-thickness shear stress. This is obtained through an efficient numerical procedure allowing the computation of both the shear stresses and the shear correction factors.

The paper is organized as follows. In Section 2, the first-order shear deformation laminate theory is reviewed together with usual techniques for the recovery of the transverse shear stresses. In Section 3 a rational procedure for the determination of the shear correction factors is proposed. In Section 4, the new 4-node laminate finite-element is developed. Because of the bending-extension coupling, the consistency of the approximations for the in-plane and transverse deformation is discussed. In Section 5, a technique for recovering the through-the-thickness shear stresses is proposed together with an iterative algorithm for the computation of the shear correction factors.

Finally, several applications are investigated to assess the performances of the proposed procedure. Results are compared with analytical FSDT solutions, exact three-dimensional solutions and other finite-element solutions.

2. FIRST-ORDER LAMINATE THEORY (FSDT)

The mechanical behaviour of a moderately thick laminate plate is herein described through a First-order Shear Deformation Theory (FSDT). The theory takes into account in-plane deformation, bending and first-order shear effects and it is briefly reviewed in the following to make the paper self-consistent.

The term laminated plate refers to a flat body, constituted by n layers of different mechanical characteristics, occupying the region:

$$\Omega = \{(x, y, z) \in \mathscr{R}^3 / z \in (-h/2, h/2),\ (x, y) \in \mathscr{A} \subset \mathscr{R}^2\} \tag{1}$$

where the plane $z = 0$ identifies the mid-surface $\mathscr{A}$ of the undeformed plate. The thickness h is assumed to be small compared to the in-plane dimensions.

Basic elements of the FSDT are: (1) the transverse stress in the thickness of the plate σ_z is null; (2) straight lines orthogonal to the midplane are inextensible and remain straight after deformation.

It is interesting to recall that in a general three-dimensional elastic theory the simultaneous presence of these two statements is formally correct and, in fact, they can be rationally introduced to obtain the FSDT for isotropic homogeneous plate.[26]

2.1. Kinematics

The plate kinematics is governed by the midplane displacements u_0, v_0, w_0 and rotations θ_x, θ_y:

$$\begin{aligned} u(x, y, z) &= u_0(x, y) + z\theta_y(x, y) \\ v(x, y, z) &= v_0(x, y) - z\theta_x(x, y) \\ w(x, y, z) &= w_0(x, y) \end{aligned} \tag{2}$$

Hence, the in-plane strain vector $\mathbf{e} = \{e_x, e_y, e_{xy}\}^{\mathrm{T}}$ can be written in the form:

$$\mathbf{e} = \boldsymbol{\varepsilon} + z\boldsymbol{\kappa} \tag{3}$$

where

$$\boldsymbol{\varepsilon} = \mathbf{E}\mathbf{u}, \quad \mathbf{E} = \begin{bmatrix} \dfrac{\partial}{\partial x} & 0 \\ 0 & \dfrac{\partial}{\partial y} \\ \dfrac{\partial}{\partial y} & \dfrac{\partial}{\partial x} \end{bmatrix}, \quad \mathbf{u} = \begin{Bmatrix} u_0 \\ v_0 \end{Bmatrix} \tag{4}$$

$$\boldsymbol{\kappa} = \mathbf{L}\boldsymbol{\theta}, \quad \mathbf{L} = \begin{bmatrix} 0 & \dfrac{\partial}{\partial x} \\ -\dfrac{\partial}{\partial y} & 0 \\ -\dfrac{\partial}{\partial x} & \dfrac{\partial}{\partial y} \end{bmatrix}, \quad \boldsymbol{\theta} = \begin{Bmatrix} \theta_x \\ \theta_y \end{Bmatrix} \tag{5}$$

Furthermore, the shear strain vector $\boldsymbol{\gamma} = \{\gamma_{xz}, \gamma_{yz}\}^{\mathrm{T}}$ is obtained by the relation:

$$\boldsymbol{\gamma} = \mathbf{W}\boldsymbol{\theta} + \nabla w, \quad \mathbf{W} = \begin{bmatrix} 0 & 1 \\ -1 & 0 \end{bmatrix}, \quad \nabla = \begin{Bmatrix} \dfrac{\partial}{\partial x} \\ \dfrac{\partial}{\partial y} \end{Bmatrix} \tag{6}$$

2.2. Local constitutive relations

The laminated composite plate is assumed to be formed by n superposed orthotropic layers with material axes arbitrarily oriented in the x–y plane.

In the generic kth layer, the following constitutive relations for the in-plane stress vector $\boldsymbol{\sigma} = \{\sigma_x, \sigma_y, \sigma_{xy}\}^{\mathrm{T}}$ and for the transverse shear stress vector $\boldsymbol{\tau} = \{\tau_{xz}, \tau_{yz}\}^{\mathrm{T}}$ hold:

$$\boldsymbol{\sigma}^{(k)} = \mathbf{Q}^{f(k)}\mathbf{e}, \quad \boldsymbol{\tau}^{(k)} = \boldsymbol{\chi}\mathbf{Q}^{t(k)}\boldsymbol{\gamma} = \widetilde{\mathbf{Q}}^{t(k)}\boldsymbol{\gamma} \tag{7}$$

where $\mathbf{Q}^{f(k)}$ is the 3×3 in-plane elastic matrix, $\mathbf{Q}^{t(k)}$ is the 2×2 shear elastic matrix, $\boldsymbol{\chi}$ is the $2 \times 2 \times 2 \times 2$ shear correction factors matrix and $\widetilde{\mathbf{Q}}^{t(k)} = \boldsymbol{\chi}\mathbf{Q}^{t(k)}$. In particular, the fourth-order matrix $\boldsymbol{\chi}$ has the following representation form:

$$\boldsymbol{\chi} = \chi_{11}\boldsymbol{\Gamma}^1 \odot \boldsymbol{\Gamma}^1 + \chi_{22}\boldsymbol{\Gamma}^2 \odot \boldsymbol{\Gamma}^2 + \chi_{12}(\boldsymbol{\Gamma}^1 \odot \boldsymbol{\Gamma}^2 + \boldsymbol{\Gamma}^2 \odot \boldsymbol{\Gamma}^1) \tag{8}$$

where

$$\boldsymbol{\Gamma}^1 = \begin{bmatrix} 1 & 0 \\ 0 & 0 \end{bmatrix}, \quad \boldsymbol{\Gamma}^2 = \begin{bmatrix} 0 & 0 \\ 0 & 1 \end{bmatrix} \tag{9}$$

and the symbol $\odot$ denotes a special matrix product, such that $(\boldsymbol{\Gamma}^i \odot \boldsymbol{\Gamma}^j)\mathbf{Q}^t = \boldsymbol{\Gamma}^i\mathbf{Q}^t\boldsymbol{\Gamma}^j$. It can be emphasized that the $\boldsymbol{\chi}$ matrix is constant along the laminate thickness, i.e. it does not change from

layer to layer, and that the values $\chi_{11}=\chi_{22}=5/6,\ \chi_{12}=0$ are correct only for an homogeneous isotropic plate.

2.3. Resultant stresses and resultant constitutive relations

The resultant stresses are defined as

$$\begin{aligned}\mathbf{N} &= \{N_x, N_y, N_{xy}\}^{\mathrm{T}} = \int_{-h/2}^{h/2} \boldsymbol{\sigma}\, \mathrm{d}z \\ \mathbf{M} &= \{M_x, M_y, M_{xy}\}^{\mathrm{T}} = \int_{-h/2}^{h/2} z\boldsymbol{\sigma}\mathrm{d}z \\ \mathbf{S} &= \{S_x, S_y\}^{\mathrm{T}} = \int_{-h/2}^{h/2} \boldsymbol{\tau}\, \mathrm{d}z\end{aligned} \tag{10}$$

The constitutive equations between the resultant stresses **N, M** and **S** and the kinematic parameters $\boldsymbol{\varepsilon}, \mathbf{k}$ and $\boldsymbol{\gamma}$ are obtained substituting the local constitutive equations (7) into the resultant stresses (10):

$$\begin{bmatrix}\mathbf{N}\\ \mathbf{M}\\ \mathbf{S}\end{bmatrix} = \begin{bmatrix}\mathbf{A} & \mathbf{B} & \mathbf{0}\\ \mathbf{B} & \mathbf{D} & \mathbf{0}\\ \mathbf{0} & \mathbf{0} & \widetilde{\mathbf{H}}\end{bmatrix} \begin{bmatrix}\boldsymbol{\varepsilon}\\ \mathbf{k}\\ \boldsymbol{\gamma}\end{bmatrix} \tag{11}$$

where $\widetilde{\mathbf{H}} = \boldsymbol{\chi}\mathbf{H}$ and the laminate stiffness matrices $\mathbf{A}, \mathbf{B}, \mathbf{D}$ and $\mathbf{H}$ are obtained by

$$\begin{aligned}\mathbf{A} &= \sum_{k=1}^{n} (z_k - z_{k-1})\mathbf{Q}^{f(k)} \qquad \mathbf{B} = \frac{1}{2}\sum_{k=1}^{n} (z_k^2 - z_{k-1}^2)\mathbf{Q}^{f(k)} \\ \mathbf{D} &= \frac{1}{3}\sum_{k=1}^{n} (z_k^3 - z_{k-1}^3)\mathbf{Q}^{f(k)} \quad \mathbf{H} = \sum_{k=1}^{n} (z_k - z_{k-1})\mathbf{Q}^{t(k)}\end{aligned} \tag{12}$$

with z_{k-1} and z_k providing the position of the kth layer in the direction of the laminate thickness.

Equation (11) highlights two interesting and well-known aspects of laminated composite plates: the coupling between bending and extension for a general lamination case and the dependence of the constitutive submatrix $\widetilde{\mathbf{H}}$ on the shear factors.

2.4. The recovering of shear stresses

Within the FSDT, the shear stresses through the thickness are often computed either using the material constitutive relations or enforcing the three-dimensional equilibrium equations. In the first case, the combination of equations (11) and $(7)_2$ gives

$$\boldsymbol{\tau}^{(k)} = \widetilde{\mathbf{Q}}^{t(k)}\widetilde{\mathbf{H}}^{-1}\mathbf{S} = \boldsymbol{\chi}\,\mathbf{Q}^{t(k)}(\boldsymbol{\chi}\,\mathbf{H})^{-1}\mathbf{S} \tag{13}$$

In the second case, the shear stress in the kth layer are

$$\widehat{\boldsymbol{\tau}}^{(k)}(z) = -\,\mathbf{E}^{\mathrm{T}} \int_{z_{k-1}}^{z} \mathbf{Q}^{f(k)}\mathbf{e}(\zeta)\ \mathrm{d}\zeta + \widehat{\boldsymbol{\tau}}_0^{(k)} \tag{14}$$

where $\widehat{\boldsymbol{\tau}}_0^{(k)}$ represents the value of the shear stress vector at $z = z_{k-1}$, i.e. $\widehat{\boldsymbol{\tau}}_0^{(k)} = \widehat{\boldsymbol{\tau}}^{(k)}(z = z_{k-1}) = \widehat{\boldsymbol{\tau}}^{(k-1)}(z = z_{k-1})$, with $\widehat{\boldsymbol{\tau}}_0^{(1)} = \mathbf{0}$. As discussed in Reference 26, this latter approach leads to a more accurate evaluation of the shear stress profile.

3. SHEAR FACTORS

A classical problem arising in conjunction with the use of the FSDT is the determination of the shear factors χ_{11}, χ_{22} and χ_{12} appearing in the matrix $\widetilde{\mathbf{H}}$ of equation (11).

The literature available on this topic shows that for laminated composite plate it is possible to determine closed-formula solutions for the χ_{ij}'s only in very special cases such as, for example, cross-ply laminates in cylindrical bending.[7]

In the following, a rational procedure for the determination of the shear correction factors in the case of a general laminate plate is proposed. It represents an extension of the classical method adopted for homogeneous isotropic plates to the case of anisotropic laminates. The procedure is based on the comparison between the shear energy computed adopting the stress vector $\boldsymbol{\tau}^{(k)}$ obtained from constitutive relations [see equation (13)] and the shear energy computed adopting the stress vector $\widehat{\boldsymbol{\tau}}^{(k)}$ recovered through three-dimensional equilibrium [see formula (14)].

In particular, the complementary shear energy per unit area $\mathscr{E}^{\mathrm{sh}}$ associated to $\boldsymbol{\tau}^{(k)}$ is defined as follows:

$$\mathscr{E}^{\mathrm{sh}} = \frac{1}{2}\int_{-h/2}^{h/2} (\boldsymbol{\tau}^{(k)})^{\mathrm{T}} (\widetilde{\mathbf{Q}}^{t(k)})^{-1} \boldsymbol{\tau}^{(k)} \mathrm{d}z = \frac{1}{2}\mathbf{S}^{\mathrm{T}} \widetilde{\mathbf{H}}^{-1} \mathbf{S} \tag{15}$$

$$= \mathscr{E}_{11}^{\mathrm{sh}} + \mathscr{E}_{22}^{\mathrm{sh}} + \mathscr{E}_{12}^{\mathrm{sh}} \tag{16}$$

where

$$\mathscr{E}_{11}^{\mathrm{sh}} = \frac{1}{2}\frac{\chi_{22} H_{22} S_x^2}{\lambda}, \quad \mathscr{E}_{22}^{\mathrm{sh}} = \frac{1}{2}\frac{\chi_{11} H_{11} S_y^2}{\lambda}, \quad \mathscr{E}_{12}^{\mathrm{sh}} = -\frac{\chi_{12} H_{12} S_x S_y}{\lambda} \tag{17}$$

with $\lambda = \chi_{11} H_{11} \chi_{22} H_{22} - \chi_{12}^2 H_{12}^2$.

Similarly, the complementary shear energy per unit area $\widehat{\mathscr{E}}^{\mathrm{sh}}$ associated to $\widehat{\boldsymbol{\tau}}$ is written as $\widehat{\mathscr{E}}^{\mathrm{sh}} = \widehat{\mathscr{E}}_{11}^{\mathrm{sh}} + \widehat{\mathscr{E}}_{22}^{\mathrm{sh}} + \widehat{\mathscr{E}}_{12}^{\mathrm{sh}}$:

$$\begin{aligned}
\widehat{\mathscr{E}}_{11}^{\mathrm{sh}} &= \frac{1}{2}\sum_{k=1}^{n}\int_{z_{k-1}}^{z_k} T_{11}^{(k)} (\widehat{\boldsymbol{\tau}}_{xz}^{(k)}(\zeta))^2 \,\mathrm{d}\zeta \\
\widehat{\mathscr{E}}_{22}^{\mathrm{sh}} &= \frac{1}{2}\sum_{k=1}^{n}\int_{z_{k-1}}^{z_k} T_{22}^{(k)} (\widehat{\boldsymbol{\tau}}_{yz}^{(k)}(\zeta))^2 \,\mathrm{d}\zeta \\
\widehat{\mathscr{E}}_{12}^{\mathrm{sh}} &= \sum_{k=1}^{n}\int_{z_{k-1}}^{z_k} T_{12}^{(k)} \widehat{\boldsymbol{\tau}}_{xz}^{(k)}(\zeta) \widehat{\boldsymbol{\tau}}_{yz}^{(k)}(\zeta) \,\mathrm{d}\zeta
\end{aligned} \tag{18}$$

with $\mathbf{T}^{(k)} = [T_{ij}^{(k)}] = (\mathbf{Q}^{t(k)})^{-1}$.

Imposing the following equalities:

$$\mathscr{E}_{11}^{\mathrm{sh}} = \widehat{\mathscr{E}}_{11}^{\mathrm{sh}}, \quad \mathscr{E}_{22}^{\mathrm{sh}} = \widehat{\mathscr{E}}_{22}^{\mathrm{sh}}, \quad \mathscr{E}_{12}^{\mathrm{sh}} = \widehat{\mathscr{E}}_{12}^{\mathrm{sh}} \tag{19}$$

a system of three equations in the three unknown shear factors is obtained:

$$\begin{aligned} \chi_{22} H_{22} S_x^2 - 2\lambda \hat{\mathscr{E}}_{11}^{\mathrm{sh}} &= 0 \\ \chi_{11} H_{11} S_y^2 - 2\lambda \hat{\mathscr{E}}_{22}^{\mathrm{sh}} &= 0 \\ \chi_{12} H_{12} S_x S_y + \lambda \hat{\mathscr{E}}_{12}^{\mathrm{sh}} &= 0 \end{aligned} \tag{20}$$

However, the energies $\hat{\mathscr{E}}_{11}^{\mathrm{sh}}$, $\hat{\mathscr{E}}_{22}^{\mathrm{sh}}$, $\hat{\mathscr{E}}_{12}^{\mathrm{sh}}$, $\mathscr{E}_{11}^{\mathrm{sh}}$, $\mathscr{E}_{22}^{\mathrm{sh}}$, $\mathscr{E}_{12}^{\mathrm{sh}}$ are functions of the actual solution state, i.e. they depend on the shear stresses $\mathbf{S}$ and on the in-plane strain state $\mathbf{e}$. Thus, in general, χ_{11}, χ_{22} and χ_{12} cannot be computed *a priori*, i.e. they can be evaluated only once the solution is obtained, which itself depends on the shear factors. Accordingly, the combination of the elastostatic problem of a composite laminate described in Section 2 with the computation of the shear factors through equations (20) results in a non-linear problem.

Finally, it can be emphasized that the computation of the χ's in a finite-element framework requires the determination of a satisfactory approximation of the resultant shear stress $\mathbf{S}$ and of the shear stress function $\hat{\boldsymbol{\tau}}^{(k)}$, which are not generally provided by standard plate finite elements.

4. A MIXED-ENHANCED FINITE ELEMENT

In this section a new finite-element for moderately thick laminate plates is proposed. The element is robust, locking free and, as shown later, it allows the recovery of the transverse shear stresses.

The following Hu–Washizu functional, with partial hybrid terms for the transverse shear, is introduced:

$$\begin{aligned} F(\mathbf{u},\boldsymbol{\theta},w,\boldsymbol{\varepsilon},\boldsymbol{\kappa},\mathbf{N},\mathbf{M},\mathbf{S}) = {} & \frac{1}{2}\int_{\mathscr{A}} \boldsymbol{\varepsilon}^{\mathrm{T}}(\mathbf{A}\boldsymbol{\varepsilon}+\mathbf{B}\boldsymbol{\kappa})\,\mathrm{d}A - \int_{\mathscr{A}} (\boldsymbol{\varepsilon}-\mathbf{E}\mathbf{u})^{\mathrm{T}}\mathbf{N}\,\mathrm{d}A \\ & + \frac{1}{2}\int_{\mathscr{A}} \boldsymbol{\kappa}^{\mathrm{T}}(\mathbf{B}\boldsymbol{\varepsilon}+\mathbf{D}\boldsymbol{\kappa})\,\mathrm{d}A - \int_{\mathscr{A}} (\boldsymbol{\kappa}-\mathbf{L}\boldsymbol{\theta})^{\mathrm{T}}\mathbf{M}\,\mathrm{d}A \\ & - \frac{1}{2}\int_{\mathscr{A}} \mathbf{S}^{\mathrm{T}}\,\widetilde{\mathbf{H}}^{-1}\mathbf{S}\,\mathrm{d}A + \int_{\mathscr{A}} \mathbf{S}^{\mathrm{T}}(\nabla w + \mathbf{W}\boldsymbol{\theta})\,\mathrm{d}A - \Pi_{\mathrm{est}} \end{aligned} \tag{21}$$

where Π_{est} describes the load and boundary potential. In the framework of incompatible modes,[27, 28] the in-plane strains are enhanced with a field $\boldsymbol{\alpha}$, such that

$$\begin{aligned} \boldsymbol{\varepsilon} &= \mathbf{E}\mathbf{u} + \boldsymbol{\alpha} \\ \boldsymbol{\kappa} &= \mathbf{L}\boldsymbol{\theta} \end{aligned} \tag{22}$$

Substituting relations (22) into functional (21),

$$\begin{aligned} H(\mathbf{u},\boldsymbol{\theta},w,\mathbf{N},\mathbf{S},\boldsymbol{\alpha}) = {} & \frac{1}{2}\int_{\mathscr{A}} (\mathbf{E}\mathbf{u}+\boldsymbol{\alpha})^{\mathrm{T}}\mathbf{A}(\mathbf{E}\mathbf{u}+\boldsymbol{\alpha})\,\mathrm{d}A - \int_{\mathscr{A}} \boldsymbol{\alpha}^{\mathrm{T}}\,\mathbf{N}\;\mathrm{d}A \\ & + \int_{\mathscr{A}} (\mathbf{E}\mathbf{u}+\boldsymbol{\alpha})^{\mathrm{T}}\mathbf{B}\mathbf{L}\boldsymbol{\theta}\,\mathrm{d}A + \frac{1}{2}\int_{\mathscr{A}} (\mathbf{L}\boldsymbol{\theta})^{\mathrm{T}}\mathbf{D}\mathbf{L}\boldsymbol{\theta}\;\mathrm{d}A \\ & - \frac{1}{2}\int_{\mathscr{A}} \mathbf{S}^{\mathrm{T}}\,\widetilde{\mathbf{H}}^{-1}\mathbf{S}\;\mathrm{d}A + \int_{\mathscr{A}} \mathbf{S}^{\mathrm{T}}(\nabla w + \mathbf{W}\boldsymbol{\theta})\;\mathrm{d}A - \Pi_{\mathrm{est}} \end{aligned} \tag{23}$$

The stationary conditions of H with respect to $\mathbf{N}$ leads to:

$$\int_{\mathscr{A}} \boldsymbol{\alpha}^{\mathrm{T}} \delta \mathbf{N} \, \mathrm{d}A = 0 \quad \Rightarrow \quad \boldsymbol{\alpha} = 0 \tag{24}$$

i.e. in solution $\boldsymbol{\varepsilon} = \mathbf{E}\mathbf{u}$.

To perform a finite-element discretization of the mixed functional (23), $\mathbf{N}$ is taken constant over each element. Thus, the discretized form of condition (24) becomes

$$\int_{\mathscr{A}_{\mathrm{e}}} \boldsymbol{\alpha} \, \mathrm{d}A = \mathbf{0} \tag{25}$$

with A_{e} the area of a generic element. Accordingly, functional (23) can be written as

$$\begin{aligned} \Pi(\mathbf{u}, w, \boldsymbol{\theta}, \mathbf{S}, \boldsymbol{\alpha}) = {} & \frac{1}{2} \int_{\mathscr{A}} (\mathbf{E}\mathbf{u} + \boldsymbol{\alpha})^{\mathrm{T}} \mathbf{A} (\mathbf{E}\mathbf{u} + \boldsymbol{\alpha}) \, \mathrm{d}A + \frac{1}{2} \int_{\mathscr{A}} (\mathbf{L}\boldsymbol{\theta})^{\mathrm{T}} \mathbf{D} \mathbf{L} \boldsymbol{\theta} \, \mathrm{d}A \\ & + \int_{\mathscr{A}} (\mathbf{L}\boldsymbol{\theta})^{\mathrm{T}} \mathbf{B} \mathbf{E} (\mathbf{u} + \boldsymbol{\alpha}) \, \mathrm{d}A - \frac{1}{2} \int_{\mathscr{A}} \mathbf{S}^{\mathrm{T}} \widetilde{\mathbf{H}}^{-1} \mathbf{S} \, \mathrm{d}A \\ & + \int_{\mathscr{A}} \mathbf{S}^{\mathrm{T}} (\nabla w + \mathbf{W}\boldsymbol{\theta}) \, \mathrm{d}A - \Pi_{\mathrm{est}} \end{aligned} \tag{26}$$

which represents an extension of the mixed functional adopted in Reference 29 for homogeneous plates to the case of anisotropic laminates.

An isoparametric four-node laminated composite element can be obtained discretizing functional (26) and considering the standard isoparametric map:[30]

$$\mathbf{x} = \begin{Bmatrix} x \\ y \end{Bmatrix} = \sum_{i=1}^{4} (1 + \xi_i \xi)(1 + \eta_i \eta) \begin{Bmatrix} x_i \\ y_i \end{Bmatrix} = \boldsymbol{\Psi} \widehat{\mathbf{x}}$$

where $\mathbf{x} = \{x, y\}^{\mathrm{T}}$ denotes the global co-ordinate vector in the physical element, $\boldsymbol{\xi} = \{\xi, \eta\}^{\mathrm{T}}$ is the local co-ordinate vector in the parent element, $\boldsymbol{\Psi}$ contains the bi-linear shape functions and $\widehat{\mathbf{x}}$ is the nodal coordinate vector.

The in-plane displacements are taken bi-linear in the nodal parameters $\widehat{\mathbf{u}}$:

$$\mathbf{u} = \boldsymbol{\Psi} \widehat{\mathbf{u}} \tag{27}$$

Following Reference 29, the transverse displacement interpolation is bi-linear in the nodal parameters $\widehat{\mathbf{w}}$, enriched with linked quadratic functions expressed in terms of the nodal rotations $\widehat{\boldsymbol{\theta}}$:

$$w = \boldsymbol{\Psi} \widehat{\mathbf{w}} + \boldsymbol{\Psi}_{w\theta} \widehat{\boldsymbol{\theta}} = \sum_{i=1}^{4} \boldsymbol{\Psi}^i \hat{w}^i - \sum_{i=1}^{4} \boldsymbol{\Psi}^i_{w\theta} L^i (\widehat{\theta}^j_n - \widehat{\theta}^i_n) \tag{28}$$

where L^i is the $i-j$ side length, $\widehat{\theta}^i_n$ and $\widehat{\theta}^j_n$ are the components of the rotations of i and j nodes in the direction normal to the $i-j$ side. The $\boldsymbol{\Psi}_{w\theta}$ shape functions are

$$\boldsymbol{\Psi}_{w\theta} = \begin{Bmatrix} \Psi^1_{w\theta} \\ \Psi^2_{w\theta} \\ \Psi^3_{w\theta} \\ \Psi^4_{w\theta} \end{Bmatrix} = \frac{1}{16} \begin{Bmatrix} (1 - \xi^2)(1 - \eta) \\ (1 + \xi)(1 - \eta^2) \\ (1 - \xi^2)(1 + \eta) \\ (1 - \xi)(1 - \eta^2) \end{Bmatrix} \tag{29}$$

The interpolation for the rotational field is bi-linear in the nodal parameters $\widehat{\boldsymbol{\theta}}$, with added internal degrees of freedom $\widehat{\boldsymbol{\theta}}_{\mathrm{b}}$:

$$\boldsymbol{\theta} = \boldsymbol{\Psi}\widehat{\boldsymbol{\theta}} + \boldsymbol{\Psi}_{\mathrm{b}}\widehat{\boldsymbol{\theta}}_{\mathrm{b}} \tag{30}$$

where $\boldsymbol{\Psi}_{\mathrm{b}}$ are bubble functions defined as

$$\boldsymbol{\Psi}_{\mathrm{b}} = \frac{(1-\xi^2)(1-\eta^2)}{j}\begin{bmatrix} J^0_{21} & -J^0_{11} & J^0_{21}\eta & -J^0_{11}\xi \\ J^0_{22} & -J^0_{12} & J^0_{22}\eta & -J^0_{12}\xi \end{bmatrix} \tag{31}$$

with $\mathbf{J}^0$ the jacobian of the iso-parametric mapping $\mathbf{J} = \partial\mathbf{x}/\partial\boldsymbol{\xi}$, evaluated at $\xi = \eta = 0$:

$$J^0_{i1} = \left.\frac{\partial x_i}{\partial \xi}\right|_{\xi=\eta=0}, \quad J^0_{i2} = \left.\frac{\partial x_i}{\partial \eta}\right|_{\xi=\eta=0}$$

and $j = \det[\mathbf{J}]$ the jacobian determinant.

The shear interpolation is

$$\mathbf{S} = \boldsymbol{\Psi}_{\mathrm{S}}\widehat{\mathbf{S}} = \begin{bmatrix} J^0_{11} & J^0_{21} & J^0_{11}\eta & J^0_{21}\xi \\ J^0_{12} & J^0_{22} & J^0_{12}\eta & J^0_{22}\xi \end{bmatrix}\begin{Bmatrix} S^1 \\ S^2 \\ S^3 \\ S^4 \end{Bmatrix} \tag{32}$$

with $\widehat{\mathbf{S}}$ parameters local to each element.

Finally, the enhanced strain $\boldsymbol{\alpha}$ is expressed as

$$\boldsymbol{\alpha} = \mathbf{G}\widehat{\boldsymbol{\alpha}} \tag{33}$$

where $\widehat{\boldsymbol{\alpha}}$ is a set of degrees of freedom local to each element and $\mathbf{G}$ is an interpolation matrix. Following Reference 28, $\mathbf{G}$ is constructed mapping an interpolation matrix $\mathbf{G}^{\mathrm{p}}$ defined on the parent element into the physical one using the formula

$$\mathbf{G} = \frac{j_0}{j}\,\mathbf{F}_0^{-\mathrm{T}}\,\mathbf{G}^{\mathrm{p}} \tag{34}$$

where j_0 is the jacobian determinant evaluated at $\xi = \eta = 0$ and

$$\mathbf{F}_0 = \begin{bmatrix} J^2_{11} & J^2_{12} & 2J_{11}J_{12} \\ J^2_{21} & J^2_{22} & 2J_{21}J_{22} \\ J_{11}J_{21} & J_{12}J_{22} & (J_{11}J_{22} + J_{12}J_{21}) \end{bmatrix}_{\xi=\eta=0} \tag{35}$$

In the following, the choice of the matrix $\mathbf{G}$ is performed taking into account two considerations. On the one hand, the enhanced strain $\boldsymbol{\alpha}$ should improve the in-plane compatible interpolation; as usual, this is done guaranteeing that the polynomial in $\mathbf{G}$ are not already contained in the compatible strains $\mathbf{Eu}$. On the other hand, the enhanced modes should satisfy an extension-bending consistency condition. In fact, due to the presence of the non-zero constitutive matrix $\mathbf{B}$ in the functional (26), the total in-plane deformation $\mathbf{Eu} + \boldsymbol{\alpha}$ is coupled with the curvature field $\mathbf{L}\boldsymbol{\theta}$. As a consequence, the in-plane and the rotation interpolations cannot be independent. In particular,

the **G** matrix should be able to satisfy the discretized form of equation $(11)_1$ for $\mathbf{N} = 0$; taking into account (22) and the interpolations (27), (30) and (33), equation $(11)_1$ reduces to

$$\mathbf{A}(\mathbf{E}\,\boldsymbol{\Psi}\,\widehat{\mathbf{u}} + \mathbf{G}\,\widehat{\boldsymbol{\alpha}}) + \mathbf{B}\,\mathbf{L}(\boldsymbol{\Psi}\,\widehat{\boldsymbol{\theta}} + \boldsymbol{\Psi}_{\mathrm{b}}\,\widehat{\boldsymbol{\theta}}_{\mathrm{b}}) = \mathbf{0} \tag{36}$$

Although equation (36) can be adopted to obtain **G** for any type of composite, in the following the discussion is limited only to cross-ply laminates. In this case, the coupling matrix assumes the following simple representation:

$$\mathbf{B} = \begin{bmatrix} b & 0 & 0 \\ 0 & -b & 0 \\ 0 & 0 & 0 \end{bmatrix}$$

with b a material constant. After some calculation, the consistency condition (36) leads to the following choice for $\mathbf{G}^{\mathrm{p}}$:

$$\mathbf{G}^{\mathrm{p}} = \begin{bmatrix} \xi & 0 & 0 & 0 & \xi\eta & \xi\eta_2 & \eta\xi_2 & \xi\eta\eta_2 & \xi\eta\xi_2 & 0 & 0 & 0 & 0 \\ 0 & \eta & 0 & 0 & -\xi\eta & 0 & 0 & 0 & 0 & \xi\eta_2 & \eta\xi_2 & \xi\eta\eta_2 & \xi\eta\xi_2 \\ 0 & 0 & \xi & \eta & \xi^2 - \eta^2 & 0 & 0 & 0 & 0 & 0 & 0 & 0 & 0 \end{bmatrix} \tag{37}$$

where $\eta_2 = 1 - \eta^2$ and $\xi_2 = 1 - \xi^2$.

Introducing the interpolation schemes (27)–(37), performing the functional stationary conditions for a single element and statically condense the enhanced strain $\widehat{\boldsymbol{\alpha}}$, the bubble rotation $\widehat{\boldsymbol{\theta}}_{\mathrm{b}}$ and the resultant shear stress $\widehat{\mathbf{S}}$, the element stiffness matrix is obtained. A detailed discussion of the procedure followed to obtain the element stiffness matrix is presented in the appendix.

The laminate element obtained is named EML4, to remember that it is an Enhanced Mixed Linked 4-node finite element.

5. IMPROVED TRANSVERSE SHEAR EFFECT

As recalled in Section 2.4, once the solution in terms of displacements has been determined, the shear stresses can be recovered using the constitutive equations (13) or enforcing the three-dimensional equilibrium equations (14) through the plate thickness. Between the two approaches, the latter returns more accurate shear stresses profiles, also if it requires the computation of the derivatives of the in-plane strains, which are usually not very accurate in classical finite element schemes (they are even zero for low order elements).

In the light of these considerations, it is interesting to point out that in the proposed EML4 the in-plane strain **e** has been properly enhanced; moreover, the adopted mixed formulation introduces the resultant stress **S** as a primary variable leading to the possibility of properly improving the shear stress profiles, as discussed next.

Taking into account equations (3), (5) and (22), the following formula for the recovery of the shear stress is proposed:

$$\widehat{\boldsymbol{\tau}}^{(k)}(z) = \begin{bmatrix} b_x & 0 \\ 0 & b_y \end{bmatrix} \left[-(z - z_{k-1})(\overline{\mathbf{P}}^{(k)}\mathbf{u} + \widehat{\mathbf{P}}^{(k)}\boldsymbol{\alpha}) - \frac{1}{2}(z^2 - z_{k-1}^2)\widetilde{\mathbf{P}}^{(k)}\boldsymbol{\theta} + \widehat{\boldsymbol{\tau}}_0^{(k)} + \mathbf{a}\left(z + \frac{h}{2}\right) \right] \tag{38}$$

where the matrices $\overline{\mathbf{P}}$, $\widehat{\mathbf{P}}$ and $\widetilde{\mathbf{P}}$ are defined as

$$\overline{\mathbf{P}}^{(k)} = \mathbf{E}^{\mathrm{T}}\mathbf{Q}^{f(k)}\mathbf{E}, \quad \widehat{\mathbf{P}}^{(k)} = \mathbf{E}^{\mathrm{T}}\mathbf{Q}^{f(k)}, \quad \widetilde{\mathbf{P}}^{(k)} = \mathbf{E}^{\mathrm{T}}\mathbf{Q}^{f(k)}\mathbf{L} \tag{39}$$

and $\widehat{\boldsymbol{\tau}}_0^{(k)}$ is the shear vector evaluated at $z = z_{k-1}$, with $\widehat{\boldsymbol{\tau}}_0^{(1)} = \mathbf{0}$.

The vector $\mathbf{a}$ and the quantities b_x and b_y are computed enforcing that the shear stress $\widehat{\boldsymbol{\tau}}^{(k)}$ evaluated at the top of the laminate is zero and that the integral of shear stress $\widehat{\boldsymbol{\tau}}^{(k)}$ over the thickness is equal to the shear stress resultant obtained from the finite element analysis. Using the notation so far introduced, these two conditions can be expressed as

$$\begin{aligned} \widehat{\boldsymbol{\tau}}^{(n)}\left(\frac{h}{2}\right) &= \mathbf{0} \Rightarrow \mathbf{a} = -\frac{1}{h}\overline{\boldsymbol{\tau}}^{(n)} \\ \sum_{k=1}^{n}\int_{z_{k-1}}^{z_k} \widehat{\boldsymbol{\tau}}^{(k)}(z)\,\mathrm{d}z &= \mathbf{S} \Rightarrow \begin{matrix} b_x = S_x/(\underline{S}_x + \overline{\tau}_{xz}^{(n)}h/2) \\ b_y = S_y/(\underline{S}_y + \overline{\tau}_{yz}^{(n)}h/2) \end{matrix} \end{aligned} \tag{40}$$

where

$$\begin{aligned} \overline{\boldsymbol{\tau}}^{(n)} &= -(z_n - z_{n-1})(\overline{\mathbf{P}}^{(n)}\mathbf{u} + \widehat{\mathbf{P}}^{(n)}\boldsymbol{\alpha}) - \frac{1}{2}(z_n^2 - z_{n-1}^2)\widetilde{\mathbf{P}}^{(n)}\boldsymbol{\theta} + \widehat{\boldsymbol{\tau}}_0^{(n)} \\ \underline{\mathbf{S}} &= \overline{\mathbf{U}}\mathbf{u} + \widehat{\mathbf{U}}\boldsymbol{\alpha} + \widetilde{\mathbf{U}}\boldsymbol{\theta} \end{aligned} \tag{41}$$

and

$$\begin{aligned} \overline{\mathbf{U}} &= -\sum_{k=1}^{n}\left[\overline{\mathbf{R}}^{(k)} + (z_k - z_{k-1})\sum_{i=1}^{k-1}\overline{\mathbf{Z}}^{(i)}\right] \\ \widehat{\mathbf{U}} &= -\sum_{k=1}^{n}\left[\widehat{\mathbf{R}}^{(k)} + (z_k - z_{k-1})\sum_{i=1}^{k-1}\widehat{\mathbf{Z}}^{(i)}\right] \\ \widetilde{\mathbf{U}} &= -\sum_{k=1}^{n}\left[\widetilde{\mathbf{R}}^{(k)} + (z_k - z_{k-1})\sum_{i=1}^{k-1}\widetilde{\mathbf{Z}}^{(i)}\right] \end{aligned} \tag{42}$$

with

$$\begin{aligned} &\overline{\mathbf{Z}}^{(k)} = (z_k - z_{k-1})\overline{\mathbf{P}}^{(k)} \qquad \overline{\mathbf{R}}^{(k)} = \tfrac{1}{2}(z_k - z_{k-1})^2\overline{\mathbf{P}}^{(k)} \\ &\widehat{\mathbf{Z}}^{(k)} = (z_k - z_{k-1})\widehat{\mathbf{P}}^{(k)} \qquad \widehat{\mathbf{R}}^{(k)} = \tfrac{1}{2}(z_k - z_{k-1})^2\widehat{\mathbf{P}}^{(k)} \\ &\widetilde{\mathbf{Z}}^{(k)} = \tfrac{1}{2}(z_k^2 - z_{k-1}^2)\widetilde{\mathbf{P}}^{(k)} \quad \widetilde{\mathbf{R}}^{(k)} = \tfrac{1}{6}(z_k^3 + 2z_{k-1}^3 - 3z_k z_{k-1}^2)\widetilde{\mathbf{P}}^{(k)} \end{aligned} \tag{43}$$

As shown in the next section, formulas (38)–(43) allow to compute very accurate shear stress profiles for both symmetrical and unsymmetrical laminated plates. Moreover, the ability to obtain accurate stress profiles opens the possibility of adopting iterative procedure for the determination of the shear factors. In the following, a procedure similar to the one proposed in Reference 12 only for very simple cases is extended to a finite-element context. In particular, the implemented iterative algorithm consists in the following steps:

1. Set an initial values for the shear factors, for example $\chi_{11} = \chi_{22} = 5/6$, $\chi_{12} = 0$.
2. Solve the FEM problem and compute the new solution $\{\widehat{\mathbf{u}}, \widehat{\mathbf{w}}, \widehat{\boldsymbol{\theta}}, \widehat{\mathbf{S}}, \widehat{\boldsymbol{\alpha}}\}$.
3. Determine the shear stresses $\widehat{\tau}_{xz}^{(k)}(z)$ and $\widehat{\tau}_{yz}^{(k)}(z)$ by equation (38).

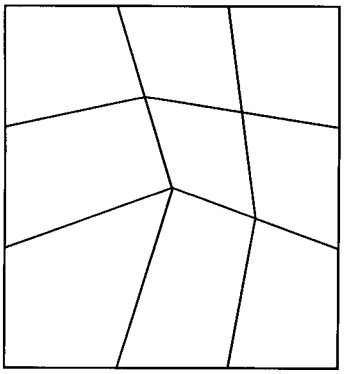

Figure 1. 3×3 unstructured mesh adopted for the laminate computations

4. Recover the shear energy in the thickness $\widehat{\mathscr{E}}^{\mathrm{sh}}_{11}$, $\widehat{\mathscr{E}}^{\mathrm{sh}}_{22}$ and $\widehat{\mathscr{E}}^{\mathrm{sh}}_{12}$ by equations (18).
5. Compute new values for the shear factors by solving the non-linear system of equations (20) for example using a Newton algorithm.
6. If the difference between the previous and the new shear factors is less than a fixed tolerance then exit, otherwise update the shear factors and go to Step 2.

6. NUMERICAL RESULTS

Several examples are now investigated to assess the performances of the new EML4 laminate element, which has been implemented in FEAP (Finite Element Analysis Program).[30]

The layer properties are set as follows:

$$E_{\mathrm{L}}/E_{\mathrm{T}} = 25, \quad \nu_{\mathrm{TT}} = 0{\cdot}25, \quad G_{\mathrm{LT}}/E_{\mathrm{T}} = 0{\cdot}5, \quad G_{\mathrm{TT}}/E_{\mathrm{T}} = 0{\cdot}2$$

corresponding to a high modulus orthotropic graphite/epoxy composite material.

6.1. *Deformation of cross-ply laminates*

The symmetric 0/90/0 and the unsymmetric 0/90 cross-ply laminates are considered. The plate is a square with side a, it is loaded either with a sinusoidal or a uniform load with maximum intensity q_0, and it is subjected to the following simply supported boundary conditions:

$$\begin{array}{l} \text{at } x = 0 \quad \text{and} \quad x = a \;\Rightarrow\; v = 0, w = 0, \theta_x = 0 \\ \text{at } y = 0 \quad \text{and} \quad y = a \;\Rightarrow\; u = 0, w = 0, \theta_y = 0 \end{array}$$

The side-to-thickness ratio is $\eta = a/h = 10$; the shear factors are constant and equal to $\chi_{11} = \chi_{22} = 5/6$, $\chi_{12} = 0$. Due to the double symmetry, only a quarter of the plate (i.e. $0 \leqslant x \leqslant a/2, 0 \leqslant y \leqslant a/2$) is studied using regular meshes as well as the unstructured meshes as the one reported in Figure 1.

For the 0/90/0 laminate, Tables I and II report the dimensionless transversal displacement $\overline{w} = 100 E_{\mathrm{T}} w / q_o h \eta^4$ at the plate centre for the sinusoidal and the uniform load, respectively. For the 0/90 laminate, Tables III and IV report the transversal displacement $\overline{w}$ at the plate centre and the

Table I. Transversal displacements $\overline{w}$ for a simply supported laminate 0/90/0 subjected to sinusoidal load: comparison between analytical and finite element solutions

Analytical solution		0·66930	
Mesh	3×3	6×6	12×12
EML4	0·66960	0·66940	0·66933
	(0·66728)	(0·66911)	(0·066927)
QUAD4	0·67080	0·66963	0·66938
	(0·65974)	(0·67011)	(0·66948)
QUAD9		0·66938	0·66931
		(0·66992)	(0·66934)

Table II. Transversal displacements $\overline{w}$ for a simply supported laminate 0/90/0 subjected to uniform load: comparison between analytical and finite element solutions

Analytical solution		1·0220	
Mesh	3×3	6×6	12×12
EML4	1·0235	1·0223	1·0220
	(1·0234)	(1·0228)	(1·0222)
QUAD4	1·0331	1·0243	1·0225
	(1·0277)	(1·0281)	(1·0234)
QUAD9		1·0222	1·0219
		(1·0232)	(1·0220)

Table III. Transversal and horizontal displacements $\overline{w}$ and $\overline{u}$ for a simply supported laminate 0/90 subjected to sinusoidal load: comparison between analytical and finite element solutions

Analytical solution		$\overline{w}$ 1·2372			$\overline{u}$ −0·078619	
Mesh	3×3	6×6	12×12	3×3	6×6	12×12
EML4	1·2370	1·2373	1·2373	−0·080466	−0·079076	−0·078733
	(1·2209)	(1·2346)	(1·2367)	(−0·079065)	(−0·078966)	(−0·078719)
QUAD4	1·2219	1·2334	1·2363	−0·078566	−0·078611	−0·078618
	(1·1927)	(1·2320)	(1·2360)	(−0·077078)	(−0·078198)	(−0·078518)
QUAD9		1·2374	1·2373		−0·078648	−0·078621
		(1·2381)	(1·2373)		(−0·078611)	(−0·078619)

Table IV. Transversal and horizontal displacements $\overline{w}$ and $\overline{u}$ for a simply supported laminate 0/90 subjected to uniform load: comparison between analytical and finite element solutions

Analytical solution		$\overline{w}$ 1·9469			$\overline{u}$ −0·129404	
Mesh	3×3	6×6	12×12	3×3	6×6	12×12
EML4	1·9481	1·9472	1·9470	−0·13241	−0·13015	−0·12959
	(1·9256)	(1·9441)	(1·9463)	(−0·12947)	(−0·12986)	(−0·12954)
QUAD4	1·9304	1·9427	1·9458	−0·12838	−0·12916	−0·12935
	(1·8971)	(1·9443)	(1·9463)	(−0·12600)	(−0·12854)	(−0·12920)
QUAD9		1·9475	1·9469		−0·12945	−0·12941
		(1·9495)	(1·9470)		(−0·12948)	(−0·12941)

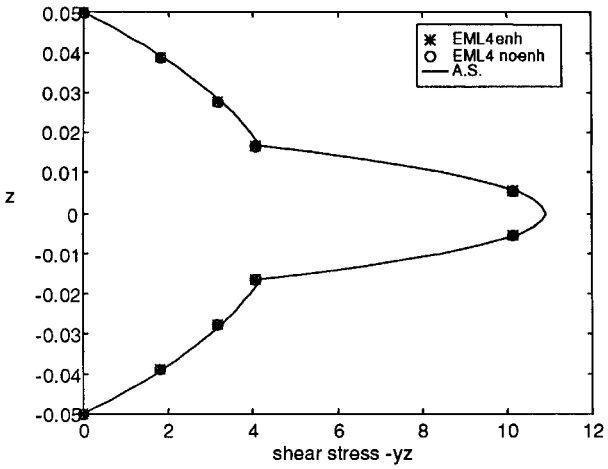

Figure 2. Shear stress $\bar{t}_{yz}$ in the thickness of the laminate 0/90/0: comparison between numerical and analytical solutions

dimensionless horizontal displacement $\bar{u} = 100E_T u/q_0 h\eta^3$ at $x = 0$ and $y = a/2$ for the sinusoidal and uniform load. The values reported in parentheses refer to the unstructured meshes.

The results from the EML4 element are compared with the analytical solution (Navier solution) and with the results obtained by the 4-node (QUAD4) and 9-node (QUAD9) elements. The QUAD4 and QUAD9 are isoparametric displacement-based elements and they require reduced integration for the shear terms to avoid locking;[30] furthermore, meshes of $n/2 \times n/2$ elements are used with the QUAD9.

The accuracy and the convergence of the EML4 numerical solutions are noted. In fact, both in-plane and out-of-plane displacement are in good accordance with the analytical solution. It can be emphasized that, although the QUAD# elements present accuracy and convergence rate comparable with the one obtained from EML4 element, they are unreliable since they suffer from locking or free energy modes. On the other hand, the new proposed element is fully robust and reliable.

6.2. Through-the-thickness shear stress profiles

The ability of the new element to compute satisfactory through-the-thickness and interlaminar shear stresses is now investigated. The square plate described above, subjected only to a sinusoidal load, is considered; the full plate is now discretized using 9×9 EML4 square elements. The shear factors are again constant and equal to $\chi_{11} = \chi_{22} = 5/6$, $\chi_{12} = 0$.

Results obtained with and without the enhanced strains are compared with the analytical solutions (AS). For the laminate 0/90/0, Figures 2 and 3 show the shear stress profiles $\bar{t}_{yz} = 100\,\hat{\tau}_{yz}/q_0\eta$ at $x = a/2$ $y = a/18$ and $\bar{t}_{xz} = 100\,\hat{\tau}_{xz}/q_0\eta$ at $x = a/18$ $y = a/2$. It is interesting to observe that no differences exist between the enhanced and the non-enhanced solution, since the transversal loading does not induce horizontal deformations and, as a consequence, the enhanced modes are non active for this problem.

Figures 4 and 5 show the shear stress profiles $\bar{t}_{yz}$ and $\bar{t}_{xz}$ for the laminate 0/90. It is interesting to observe that now there is a significative improvement between the enhanced and the non-enhanced solution; in fact, the transversal loading does induce horizontal deformations in the 0/90 laminate and, accordingly, the enhanced modes are now active and produce an improvement of the solution.

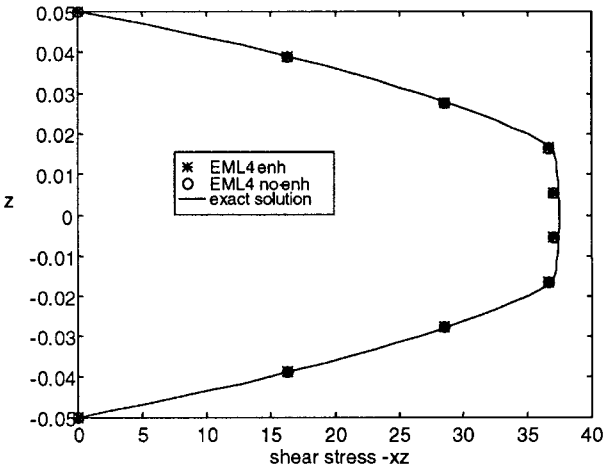

Figure 3. Shear stress $\bar{t}_{xz}$ in the thickness of the laminate 0/90/0: comparison between numerical and analytical solutions

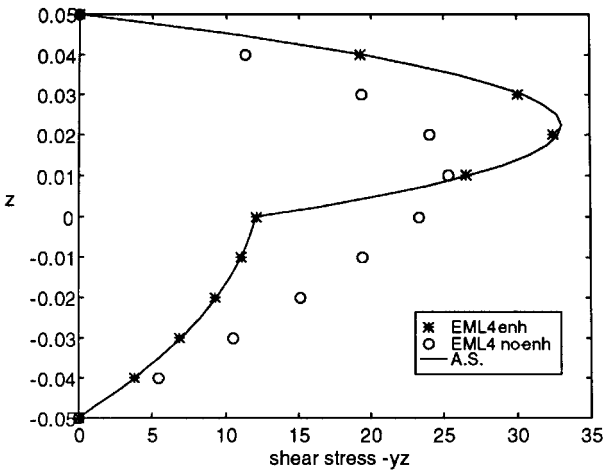

Figure 4. Shear stress $\bar{t}_{yz}$ in the thickness of the laminate 0/90: comparison between numerical and analytical solutions

The excellent approximation of the shear stresses computed by the EML4 with respect to the analytical solution is noted, in particular for the more difficult case of the unsymmetric laminate.

Then, the shear stress profile $\bar{t}_{yz}$ at $x = a/2$ $y = 0$ for the 0/90/0 laminate with side-to-thickness ratio $\eta = 4$, considered in References 22 and 23 is reported in Figure 6 to compare the solution provided by the proposed EML4 element and the one obtained by the QHD40 continuum element developed in References 20 and 21. Figure 6 shows that EML4 gives more accurate results with respect to QHD40.

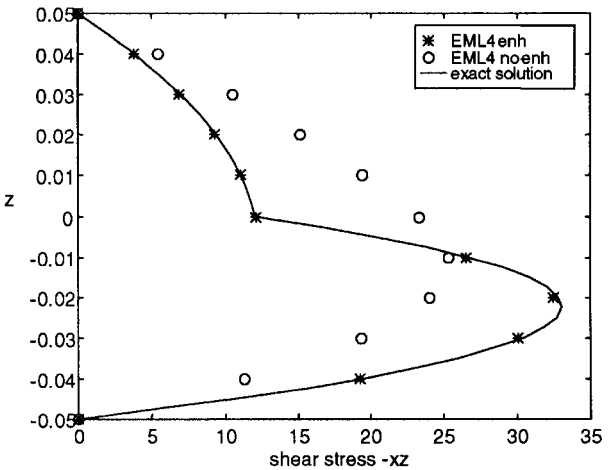

Figure 5. Shear stress $\bar{t}_{xz}$ in the thickness of the laminate 0/90: comparison between numerical and analytical solutions

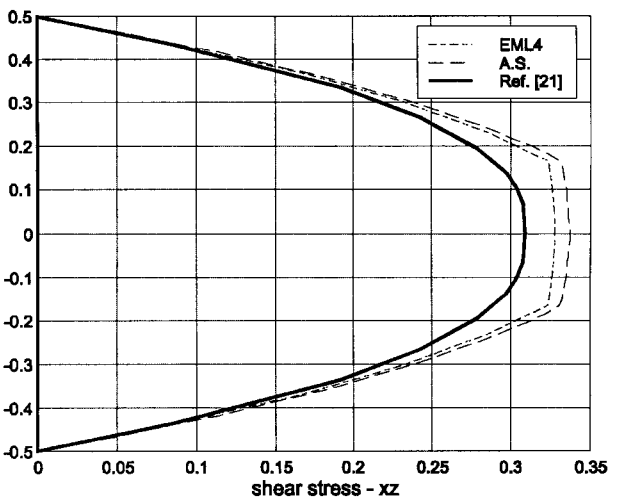

Figure 6. Comparison between the shear stress computed using the EML4, the QHD40[20] and the analytical solution

6.3. *Shear factors determination*

The procedure proposed in Section 5 is now applied to obtain the correct shear factors. Both symmetric and unsymmetric cross-ply laminates in cylindrical bending are investigated. A laminated strip is discretized using 1×10 elements.

In Table V the finite-element results are compared with the exact solution.[9, 10] It can be noted that the numerical results are in excellent agreement with the analytical solutions for all the different laminations considered. The values of the shear factors reported in Table V are obtained by performing only two iterations, for all the considered laminates. In fact, since laminates in cylindrical bending are statically determined structures, the shear stress profiles are computed

Table V. Shear correction factors: comparison between analytical and numerical results

	0/90/90/0		0/90		$((0/90)_5)_s$	
	χ_{11}	χ_{22}	χ_{11}	χ_{22}	χ_{11}	χ_{22}
AS	0·5952	0·7205	0·8212	0·8212	0·6784	0·6693
EML4	0·5951	0·7224	0·8222	0·8222	0·6784	0·6697

Table VI. Transversal diplacements $\overline{w}$ for cross-ply laminates in cylindrical bending

	0/90/0	0/90
EML4_i	356·77	1233·4
EML4_f	421·30	1234·9
	$\chi_{11} = 0{\cdot}5826$	$\chi_{11} = 0{\cdot}8281$
3D-elasticity	417·27	1243·8

independently from the displacement solution, and thus the shear factors are recovered once the shear stresses are given.

6.4. *Shear factor effects*

The improvement of the 2D plate solution versus the 3D solution due to the use of the correct shear factors is now demonstrated.

Two plates are considered, respectively with a 0/90/0 and a 0/90 lamination. The plates are simply supported along two edges and are subjected to a uniform line-load applied at the mid-span. Because of the structural scheme symmetry and of the cylindrical bending conditions, only half strip is discretized using 1×10 elements.

Table VI shows the maximum transversal displacement $\overline{w}$ obtained from EML4 with shear factors equal to 5/6 (_i) and with the shear factors obtained through the iterative procedure described in Section 5 (_f). The plate solutions are compared also with 3D finite-element solutions obtained using a mesh of $12 \times 20 \times 1$ 3D orthotropic elements in a plane strain condition. It can be emphasized the significative improvement of the solution, when the iterative procedure for the computation of the shear factors is applied, in particular for the 0/90/0 lamination. The shear factor values at the end of the iterative procedure are reported in Table VI.

Figures 7 and 8 show the tangential stress profiles computed at $x = a/8$ for the 0/90/0 and 0/90 laminations, respectively, together with the shear stress profile obtained by the 3D solution. Also in this case, the accuracy of the EML4 numerical solution can be noted.

As emphasized in the previous subsection, for laminates in cylindrical bending the shear factors are computed by performing only two iterations.

6.5. *Shear factor distributions*

As final computations, two simply supported square 0/90/90/0 laminates, subjected respectively to a uniform load and to a point-wise force at the centre of the plate, are studied. The goal is to show the variation of the shear correction factors within the plate.

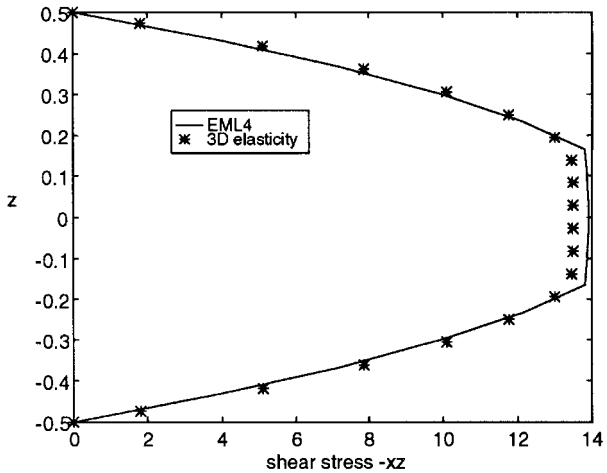

Figure 7. Shear stress in the thickness of a laminate 0/90/0 in cylindrical bending: comparison between EML4 and 3D elasticity solutions

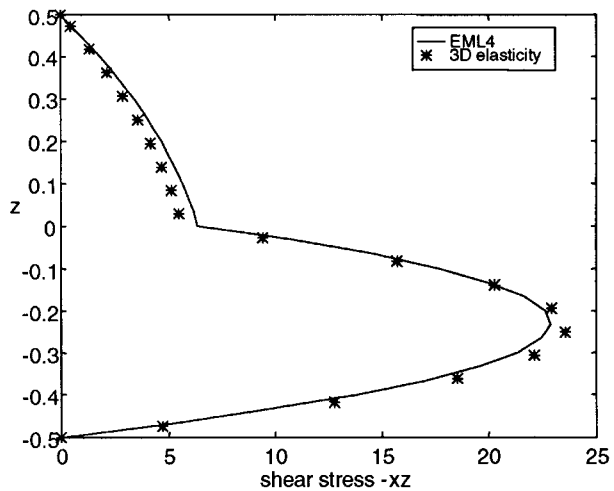

Figure 8. Shear stress in the thickness of a laminate 0/90 in cylindrical bending: comparison between EML4 and 3D elasticity solutions

Due to the plate double symmetry, only a quarter of the plate (i.e. $0 \leqslant x \leqslant a/2, 0 \leqslant y \leqslant a/2$) is studied using regular 9×9 meshes. The χ_{11} and χ_{22} contour plots are shown in Figures 9 and 10, for the uniform load, and in Figures 11 and 12, for the point-wise force. It can be noted how both χ_{11} and χ_{22} are not constant within the plate.

To obtain satisfactory values for the shear factors several iterations are necessary for the analysed structures. In particular, it is necessary to perform 10 iterations for the case of distributed loading, and 12 iterations for the case of point-wise force.

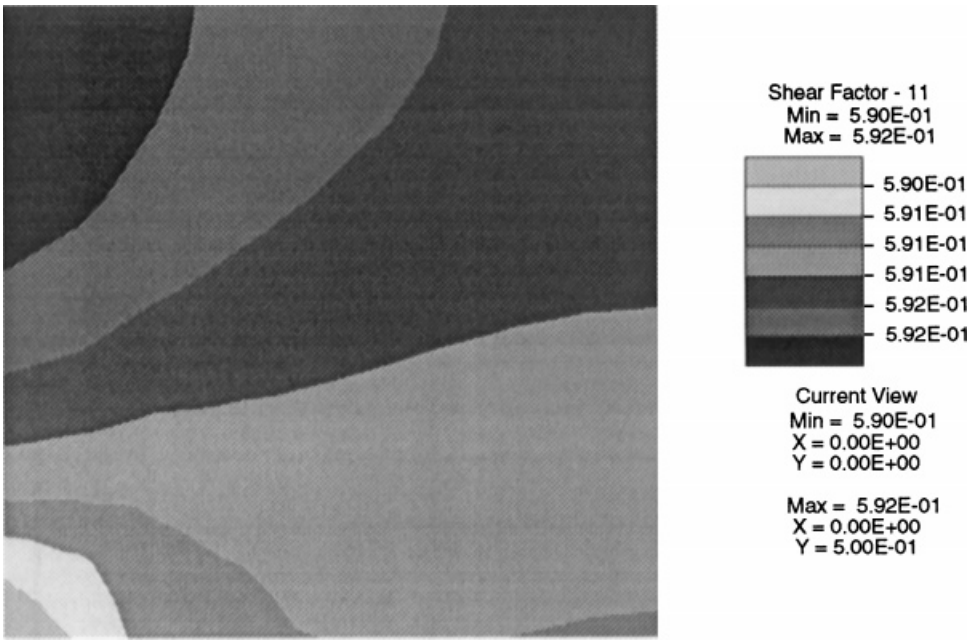

Figure 9. Contour plot of the shear factor χ_{11} for a simply supported square laminate 0/90/90/0 subjected to a uniform load

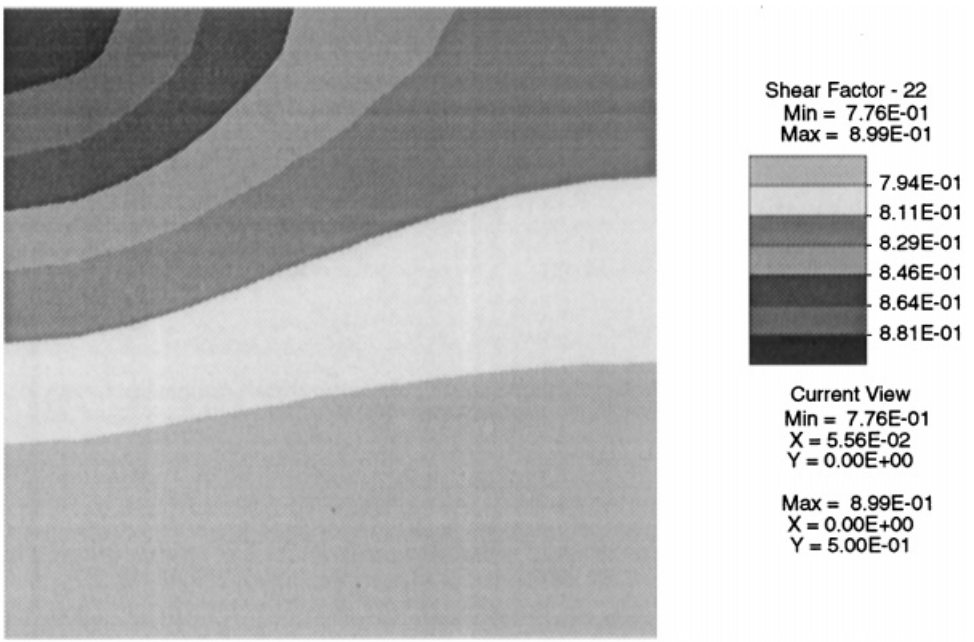

Figure 10. Contour plot of the shear factor χ_{22} for a simply supported square laminate 0/90/90/0 subjected to a uniform load

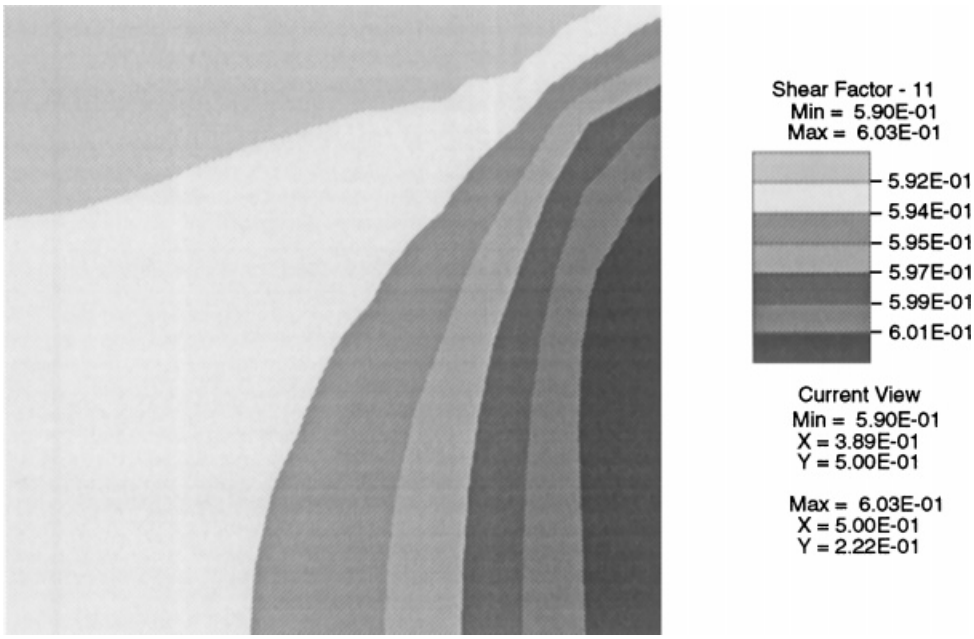

Figure 11. Contour plot of the shear factor χ_{11} for a simply supported square laminate 0/90/90/0 subjected to a point-wise central force

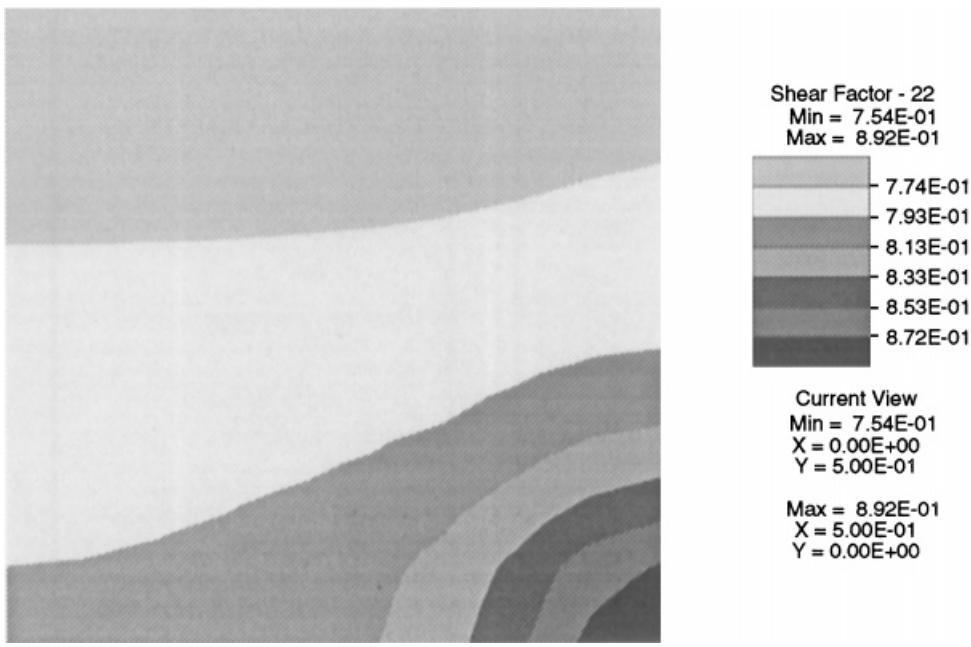

Figure 12. Contour plot of the shear factor χ_{22} for a simply supported square laminate 0/90/90/0 subjected to a point-wise central force

7. CONCLUDING REMARKS

A new advanced finite-element for the analysis of laminated plates has been proposed. Starting from a first-order shear deformation theory and adopting a mixed-enhanced variational formulation, the element is constructed using bubble functions for the rotational degrees of freedom, functions linking the transverse displacement to the rotations and enhanced modes for the in-plane deformations.

Furthermore, a procedure for the computation of the through-the-thickness shear stresses is discussed, together with an iterative algorithm for an accurate evaluation of the shear correction factors.

Several applications are investigated and results are compared with analytical solutions as well as with other 2D and 3D finite-element solutions.

The reported numerical examples highlight that the new element provides very accurate in-plane/out-of-plane displacements, especially when the shear factors are properly computed. At the same time, it is shown how the shear factors may vary quite significantly within the domain of a classical problem, aspect which underlines the need of a shear factor evaluation procedure within a finite-element framework, as the one developed here.

The ability to compute very accurate shear stress profiles for both symmetric and unsymmetric laminated plates is also assessed. The recovery of accurate stress profiles is of crucial importance, since they are often responsible for the activation and the development of delamination mechanisms. In particular, delamination can occur close to the edges of laminates, where initial defects could be present and where applied loads could induce high values of the resultant shear. On the other hand, once the shear stress profiles are known, it could be possible to develope also a technique able to recover the normal stress in the laminate thickness by through-the-thickness integration of the shear stresses. Accordingly, the new finite-element here proposed opens the possibility of interesting future work, directed toward the modelling of delamination effects.

APPENDIX

Introducing the interpolation schemes (27)–(37) in functional (26) and performing the stationary conditions for a single element, the following algebraic system is obtained:

$$\begin{bmatrix} \mathbf{K}_{uu} & \mathbf{0} & \mathbf{K}_{u\theta} & \mathbf{K}_{ub} & \mathbf{0} & \mathbf{K}_{\alpha u}^{\mathrm{T}} \\ \mathbf{0} & \mathbf{0} & \mathbf{0} & \mathbf{0} & \mathbf{K}_{Sw}^{\mathrm{T}} & \mathbf{0} \\ \mathbf{K}_{u\theta}^{\mathrm{T}} & \mathbf{0} & \mathbf{K}_{\theta\theta} & \mathbf{K}_{b\theta}^{\mathrm{T}} & \mathbf{K}_{S\theta}^{\mathrm{T}} & \mathbf{K}_{\alpha\theta}^{\mathrm{T}} \\ \mathbf{K}_{ub}^{\mathrm{T}} & \mathbf{0} & \mathbf{K}_{b\theta} & \mathbf{K}_{bb} & \mathbf{K}_{bS} & \mathbf{K}_{\alpha b}^{\mathrm{T}} \\ \mathbf{0} & \mathbf{K}_{Sw} & \mathbf{K}_{S\theta} & \mathbf{K}_{bS}^{\mathrm{T}} & \mathbf{K}_{SS} & \mathbf{0} \\ \mathbf{K}_{\alpha u} & \mathbf{0} & \mathbf{K}_{\alpha\theta} & \mathbf{K}_{\alpha b} & \mathbf{0} & \mathbf{K}_{\alpha\alpha} \end{bmatrix} \begin{Bmatrix} \widehat{\mathbf{u}} \\ \widehat{\mathbf{w}} \\ \widehat{\boldsymbol{\theta}} \\ \widehat{\boldsymbol{\theta}}_{\mathrm{b}} \\ \widehat{\mathbf{S}} \\ \widehat{\boldsymbol{\alpha}} \end{Bmatrix} = \begin{Bmatrix} \widehat{\mathbf{f}}_u \\ \widehat{\mathbf{f}}_w \\ \widehat{\mathbf{f}}_\theta \\ \mathbf{0} \\ \mathbf{0} \\ \mathbf{0} \end{Bmatrix} \tag{44}$$

where the right-hand side contains the terms due to loads and boundary conditions. The submatrices in (44) are given by

$$\mathbf{K}_{uu} = \int_{\mathscr{A}_e} (\mathbf{E}\boldsymbol{\Psi})^{\mathrm{T}} \mathbf{A} \mathbf{E} \boldsymbol{\Psi} \, \mathrm{d}A \quad \mathbf{K}_{u\theta} = \int_{\mathscr{A}_e} (\mathbf{E}\boldsymbol{\Psi})^{\mathrm{T}} \mathbf{B} \mathbf{L} \boldsymbol{\Psi} \, \mathrm{d}A$$

$$\mathbf{K}_{\theta\theta} = \int_{\mathscr{A}_e} (\mathbf{L}\boldsymbol{\Psi})^{\mathrm{T}} \mathbf{D} \mathbf{L} \boldsymbol{\Psi} \, \mathrm{d}A \quad \mathbf{K}_{bu} = \int_{\mathscr{A}_e} (\mathbf{L}\boldsymbol{\Psi}_b)^{\mathrm{T}} \mathbf{B} \mathbf{E} \boldsymbol{\Psi} \, \mathrm{d}A$$

$$\mathbf{K}_{b\theta} = \int_{\mathscr{A}_e} (\mathbf{L}\boldsymbol{\Psi}_b)^{\mathrm{T}} \mathbf{D}\mathbf{L}\boldsymbol{\Psi} \,\mathrm{d}A \qquad \mathbf{K}_{bb} = \int_{\mathscr{A}_e} (\mathbf{L}\boldsymbol{\Psi}_b)^{\mathrm{T}} \mathbf{D}\mathbf{L}\boldsymbol{\Psi}_b \,\mathrm{d}A$$

$$\mathbf{K}_{bS} = -\int_{\mathscr{A}_e} \boldsymbol{\Psi}_b^{\mathrm{T}} \mathbf{W}\boldsymbol{\Psi}_S \,\mathrm{d}A \qquad \mathbf{K}_{Sw} = \int_{\mathscr{A}_e} \boldsymbol{\Psi}_S^{\mathrm{T}} \nabla\boldsymbol{\Psi} \,\mathrm{d}A$$

$$\mathbf{K}_{S\theta} = \int_{\mathscr{A}_e} \boldsymbol{\Psi}_S^{\mathrm{T}} ([\nabla\boldsymbol{\Psi}_{w\theta}] + \mathbf{W}\boldsymbol{\Psi}) \,\mathrm{d}A \qquad \mathbf{K}_{SS} = -\int_{\mathscr{A}_e} \boldsymbol{\Psi}_S^{\mathrm{T}} \widetilde{\mathbf{H}}^{-1} \boldsymbol{\Psi}_S \,\mathrm{d}A$$

$$\mathbf{K}_{\alpha u} = \int_{\mathscr{A}_e} \mathbf{G}^{\mathrm{T}} \mathbf{A}\mathbf{E}\boldsymbol{\Psi} \,\mathrm{d}A \qquad \mathbf{K}_{\alpha\theta} = \int_{\mathscr{A}_e} \mathbf{G}^{\mathrm{T}} \mathbf{B}\mathbf{L}\boldsymbol{\Psi} \,\mathrm{d}A$$

$$\mathbf{K}_{\alpha b} = \int_{\mathscr{A}_e} \mathbf{G}^{\mathrm{T}} \mathbf{B}\mathbf{L}\boldsymbol{\Psi}_b \,\mathrm{d}A \qquad \mathbf{K}_{\alpha\alpha} = \int_{\mathscr{A}_e} \mathbf{G}^{\mathrm{T}} \mathbf{A}\mathbf{G} \,\mathrm{d}A$$

Recalling that the enhanced strain $\widehat{\boldsymbol{\alpha}}$, the bubble rotation $\widehat{\boldsymbol{\theta}}_{\mathrm{b}}$ and the resultant shear stress $\widehat{\mathbf{S}}$ are parameters local to each element, they can be eliminated by static condensation.

The condensation with respect to the enhanced degrees of freedom $\widehat{\boldsymbol{\alpha}}$ leads to:

$$\begin{bmatrix} \underline{\mathbf{K}}_{uu} & \mathbf{0} & \underline{\mathbf{K}}_{u\theta} & \underline{\mathbf{K}}_{bu}^{\mathrm{T}} & \mathbf{0} \\ \mathbf{0} & \mathbf{0} & \mathbf{0} & \mathbf{0} & \underline{\mathbf{K}}_{Sw}^{\mathrm{T}} \\ \underline{\mathbf{K}}_{u\theta}^{\mathrm{T}} & \mathbf{0} & \underline{\mathbf{K}}_{\theta\theta} & \underline{\mathbf{K}}_{b\theta}^{\mathrm{T}} & \underline{\mathbf{K}}_{S\theta}^{\mathrm{T}} \\ \underline{\mathbf{K}}_{bu} & \mathbf{0} & \underline{\mathbf{K}}_{b\theta} & \underline{\mathbf{K}}_{bb} & \underline{\mathbf{K}}_{bS} \\ \mathbf{0} & \underline{\mathbf{K}}_{Sw} & \underline{\mathbf{K}}_{S\theta} & \underline{\mathbf{K}}_{bS}^{\mathrm{T}} & \underline{\mathbf{K}}_{SS} \end{bmatrix} \begin{Bmatrix} \widehat{\mathbf{u}} \\ \widehat{\mathbf{w}} \\ \widehat{\boldsymbol{\theta}} \\ \widehat{\boldsymbol{\theta}}_b \\ \widehat{\mathbf{S}} \end{Bmatrix} = \begin{Bmatrix} \widehat{\mathbf{f}}_u \\ \widehat{\mathbf{f}}_w \\ \widehat{\mathbf{f}}_\theta \\ \mathbf{0} \\ \mathbf{0} \end{Bmatrix} \tag{45}$$

where

$$\underline{\mathbf{K}}_{uu} = \mathbf{K}_{uu} - \mathbf{K}_{\alpha u}^{\mathrm{T}} \mathbf{K}_{\alpha\alpha}^{-1} \mathbf{K}_{\alpha u} \qquad \underline{\mathbf{K}}_{u\theta} = \mathbf{K}_{u\theta} - \mathbf{K}_{\alpha u}^{\mathrm{T}} \mathbf{K}_{\alpha\alpha}^{-1} \mathbf{K}_{\alpha\theta}$$
$$\underline{\mathbf{K}}_{\theta\theta} = \mathbf{K}_{\theta\theta} - \mathbf{K}_{\alpha\theta}^{\mathrm{T}} \mathbf{K}_{\alpha\alpha}^{-1} \mathbf{K}_{\alpha\theta} \qquad \underline{\mathbf{K}}_{bu} = \mathbf{K}_{bu} - \mathbf{K}_{\alpha b}^{\mathrm{T}} \mathbf{K}_{\alpha\alpha}^{-1} \mathbf{K}_{\alpha u}$$
$$\underline{\mathbf{K}}_{b\theta} = \mathbf{K}_{b\theta} - \mathbf{K}_{\alpha b}^{\mathrm{T}} \mathbf{K}_{\alpha\alpha}^{-1} \mathbf{K}_{\alpha\theta} \qquad \underline{\mathbf{K}}_{bb} = \mathbf{K}_{bb} - \mathbf{K}_{\alpha b}^{\mathrm{T}} \mathbf{K}_{\alpha\alpha}^{-1} \mathbf{K}_{\alpha b}$$
$$\underline{\mathbf{K}}_{bS} = \mathbf{K}_{bS} \qquad \underline{\mathbf{K}}_{Sw} = \mathbf{K}_{Sw}$$
$$\underline{\mathbf{K}}_{S\theta} = \mathbf{K}_{S\theta} \qquad \underline{\mathbf{K}}_{SS} = \mathbf{K}_{SS}$$

When the internal rotational degrees of freedom are eliminated by static condensation, the following reduced stiffness matrix is obtained:

$$\begin{bmatrix} \widetilde{\mathbf{K}}_{uu} & \mathbf{0} & \widetilde{\mathbf{K}}_{u\theta} & \widetilde{\mathbf{K}}_{Su}^{\mathrm{T}} \\ \mathbf{0} & \mathbf{0} & \mathbf{0} & \widetilde{\mathbf{K}}_{wS}^{\mathrm{T}} \\ \widetilde{\mathbf{K}}_{u\theta}^{\mathrm{T}} & \mathbf{0} & \widetilde{\mathbf{K}}_{\theta\theta} & \widetilde{\mathbf{K}}_{S\theta}^{\mathrm{T}} \\ \widetilde{\mathbf{K}}_{Su} & \widetilde{\mathbf{K}}_{Sw} & \widetilde{\mathbf{K}}_{S\theta} & \widetilde{\mathbf{K}}_{SS} \end{bmatrix} \begin{Bmatrix} \widehat{\mathbf{u}} \\ \widehat{\mathbf{w}} \\ \widehat{\boldsymbol{\theta}} \\ \widehat{\mathbf{S}} \end{Bmatrix} = \begin{Bmatrix} \widehat{\mathbf{f}}_u \\ \widehat{\mathbf{f}}_w \\ \widehat{\mathbf{f}}_\theta \\ \mathbf{0} \end{Bmatrix} \tag{46}$$

where

$$\widetilde{\mathbf{K}}_{uu} = \underline{\mathbf{K}}_{uu} - \underline{\mathbf{K}}_{bu}^{\mathrm{T}}\underline{\mathbf{K}}_{bb}^{-1}\underline{\mathbf{K}}_{bu} \quad \widetilde{\mathbf{K}}_{u\theta} = \underline{\mathbf{K}}_{u\theta} - \underline{\mathbf{K}}_{bu}^{\mathrm{T}}\underline{\mathbf{K}}_{bb}^{-1}\underline{\mathbf{K}}_{b\theta}$$

$$\widetilde{\mathbf{K}}_{\theta\theta} = \underline{\mathbf{K}}_{\theta\theta} - \underline{\mathbf{K}}_{b\theta}^{\mathrm{T}}\underline{\mathbf{K}}_{bb}^{-1}\underline{\mathbf{K}}_{b\theta} \quad \widetilde{\mathbf{K}}_{Su} = -\underline{\mathbf{K}}_{bS}^{\mathrm{T}}\underline{\mathbf{K}}_{bb}^{-1}\underline{\mathbf{K}}_{bu}$$

$$\widetilde{\mathbf{K}}_{Sw} = \underline{\mathbf{K}}_{Sw} \quad \widetilde{\mathbf{K}}_{S\theta} = \underline{\mathbf{K}}_{S\theta} - \underline{\mathbf{K}}_{bS}^{\mathrm{T}}\underline{\mathbf{K}}_{bb}^{-1}\underline{\mathbf{K}}_{b\theta}$$

$$\widetilde{\mathbf{K}}_{SS} = \underline{\mathbf{K}}_{SS} - \underline{\mathbf{K}}_{bS}^{\mathrm{T}}\underline{\mathbf{K}}_{bb}^{-1}\underline{\mathbf{K}}_{bS}$$

Furthermore, if the shear parameters are also eliminated, the final element stiffness matrix is obtained:

$$\begin{bmatrix} \overline{\mathbf{K}}_{uu} & \overline{\mathbf{K}}_{uw} & \overline{\mathbf{K}}_{u\theta} \\ \overline{\mathbf{K}}_{uw}^{\mathrm{T}} & \overline{\mathbf{K}}_{ww} & \overline{\mathbf{K}}_{w\theta} \\ \overline{\mathbf{K}}_{u\theta}^{\mathrm{T}} & \overline{\mathbf{K}}_{w\theta}^{\mathrm{T}} & \overline{\mathbf{K}}_{\theta\theta} \end{bmatrix} \begin{Bmatrix} \widehat{\mathbf{u}} \\ \widehat{\mathbf{w}} \\ \widehat{\boldsymbol{\theta}} \end{Bmatrix} = \begin{Bmatrix} \widehat{\mathbf{f}}_u \\ \widehat{\mathbf{f}}_w \\ \widehat{\mathbf{f}}_\theta \end{Bmatrix} \tag{47}$$

where

$$\overline{\mathbf{K}}_{uu} = \widetilde{\mathbf{K}}_{uu} - \widetilde{\mathbf{K}}_{Su}^{\mathrm{T}}\widetilde{\mathbf{K}}_{SS}^{-1}\widetilde{\mathbf{K}}_{Su} \quad \overline{\mathbf{K}}_{uw} = -\widetilde{\mathbf{K}}_{Su}^{\mathrm{T}}\widetilde{\mathbf{K}}_{SS}^{-1}\widetilde{\mathbf{K}}_{Sw}$$

$$\overline{\mathbf{K}}_{u\theta} = \widetilde{\mathbf{K}}_{u\theta} - \widetilde{\mathbf{K}}_{Su}^{\mathrm{T}}\widetilde{\mathbf{K}}_{SS}^{-1}\widetilde{\mathbf{K}}_{S\theta} \quad \overline{\mathbf{K}}_{ww} = -\widetilde{\mathbf{K}}_{wS}^{\mathrm{T}}\widetilde{\mathbf{K}}_{SS}^{-1}\widetilde{\mathbf{K}}_{Sw}$$

$$\overline{\mathbf{K}}_{w\theta} = -\widetilde{\mathbf{K}}_{wS}^{\mathrm{T}}\widetilde{\mathbf{K}}_{SS}^{-1}\widetilde{\mathbf{K}}_{S\theta} \quad \overline{\mathbf{K}}_{\theta\theta} = \widetilde{\mathbf{K}}_{\theta\theta} - \widetilde{\mathbf{K}}_{\theta S}\widetilde{\mathbf{K}}_{SS}^{-1}\widetilde{\mathbf{K}}_{S\theta}$$

It is worth noting that the invertibility of $\mathbf{K}_{SS}$ is not required during the algebraic manipulations. On the contrary, it is necessary to compute the inverse of $\widetilde{\mathbf{K}}_{SS}$, which is not singular even for zero shear compliance. This is obtained by proper selection of the shape bubble functions. Any problem converging to the thin plate case can be investigated, without the problem becoming ill-conditioned; similarly, the shear energy can be included or excluded from the analysis as an optional element feature.

In the construction of the stiffness matrix (44), the contribution of $\mathbf{K}_{ub}$ and $\mathbf{K}_{\alpha b}$ is ignored in order to satisfy the consistency condition (36) also for the case of distorted elements.

ACKNOWLEDGEMENTS

The financial supports of the Italian National Research Council (CNR), of the Ministry of University and Research (MURST) and of the Italian Space Agency (ASI) are gratefully acknowledged.

REFERENCES

1. E. Reissner and Y. Stavsky, 'Bending and stretching of certain types of heterogeneous aelotropic elastic plates', *J. Appl. Mech.*, **28,** 402–412 (1961).
2. Y. Stavsky, 'Bending and stretching of laminated aelotropic plates', *Proc. Am. Soc. Civil Engrs.*, **87,** 31–42 (1961).
3. E. Reissner, 'The effect of transverse shear deformation on the bending of elastic plates', *J. Appl. Mech.*, **12,** 69–77 (1945).
4. R. D. Mindlin, 'Influence of rotatory inertia and shear on flexural motions of isotropic, elastic plates', *J. Appl. Mech.*, **38,** 31–38 (1951).
5. P. C. Yang, C. H. Norris and Y. Stavsky, 'Elastic wave propagation in heterogeneous plates', *Int. J. Solids Struct.*, **2,** 665–684 (1966).
6. J. M. Whitney and N. J. Pagano, 'Shear deformation in heterogeneous anisotropic plates', *J. Appl. Mech.*, *Trans. ASME* 92/E, **37,** 1031–1036 (1970).
7. J. M. Whitney, 'Shear correction factors for orthotropic laminates under static load', *J. Appl. Mech.*, **40,** 302–304 (1973).

8. S. Vlachoutsis, 'Shear correction factor for plates and shells', *Int. J. Numer. Meth. Engng.*, **33,** 1537–1552 (1992).
9. M. Laitinen, H. Lahtinen and S.-G. Sjölind, 'Transverse shear correction factors for laminates in cylindrical bending', *Comm. Numer. Meth. Engng.*, **11,** 41–47 (1995).
10. A. K. Noor and W. S. Burton, 'Stress and free vibration analyses of multilayered composite plates', *Comput. Struct.*, **11,** 183–204 (1989).
11. A. K. Noor and W. S. Burton, 'Assessment of computational models for multilayered anisotropic plates', *Comput. Struct.*, **14,** 233–265 (1990).
12. A. K. Noor, W. S. Burton and J. M. Peters, 'Predictor-corrector procedures for stress and free vibration analyses of multilayered composite plates and shells', *Int. J. Comp. Meth. Appl. Mech. Engng.*, **82,** 341–363 (1990).
13. P. F. Pai, 'A new look at the shear correction factors and warping functions of anisotropic laminates', *Int. J. Solids Struct.*, **32,** 2295–2313 (1995).
14. Y. Qi and N. F. Knight Jr, 'A refined first-order shear-deformation theory and its justification by plane-strain bending problem of laminated plates', *Int. J. Solids Struct.*, **33,** 49–64 (1996).
15. K. H. Lo, R. M. Christensen and E. M. Wu, 'A high-order theory of plate deformation. Part II: laminated plates', *J. Appl. Mech.*, **44,** 669–676 (1978).
16. J. N. Reddy, 'A simple higher-order theory for laminated composite plates', *J. Appl. Mech.*, **51,** 745–752 (1984).
17. J. N. Reddy, 'A generalization of two-dimensional theories of laminated plates', *Comm. Appl. Numer. Meth.*, **3,** 173–180 (1987).
18. M. Di Sciuva, 'An improved shear deformation theory for moderately thick multilayered anisotropic shells and plates', *J. Appl. Mech.*, **54,** 589–596 (1987).
19. P. Bisegna and E. Sacco, 'A layer-wise laminate theory rationally deduced from three-dimensional elasticity', *J. Appl. Mech.*, in press.
20. O. O. Ochoa and J. N. Reddy, *Finite Element Analysis of Composite Laminates*, Kluwer Academic Publishers, Dordrecht, 1992.
21. J. J. Engblom and O. O. Ochoa, 'Through-the-thickness stress distribution for laminated plates of advanced composite materials', *Int. J. Numer. Meth. Engng.*, **21,** 1759–1776 (1985).
22. R. L. Spilker, 'Hybrid-stress eight-node element for thin and thick multilayered laminated plates', *Int. J. Numer. Meth. Engng.*, **18,** 801–828 (1982).
23. W. Liou and C. T. Sun, 'A three-dimensional hybrid stress isoparametric element for the analysis of laminated composite plates', *Comput. Struct.*, **25,** 241–249 (1987).
24. Y. K. Yong and Y. Cho, 'Higher-order, partial hybrid stress, finite element formulation for laminated plate and shells analyses', *Comput. Struct.*, **57,** 817–827 (1995).
25. E. J. Barbero, 'A 3-d finite element for laminated composites with 2-d kinematic constraints', *Comput. Struct.*, **45,** 263–271 (1992).
26. P. Bisegna and E. Sacco 'A rational deduction of plate theories from the three-dimensional linear elasticity', *Zeit. Für Angew. Math. Mech.*, in press.
27. T. H. H. Pian and K. Sumihara, 'Rational approach for assumed stress finite elements', *Int. J. Numer. Meth. Engng.*, **20,** 1685–1695 (1984).
28. J. C. Simo and M. S. Rifai, 'A class of mixed assumed strain methods and the method of incompatible modes', *Int. J. Numer. Meth. Engng.*, **29,** 1595–1638 (1990).
29. F. Auricchio and R. L. Taylor, 'A shear deformable plate element with an exact thin limit', *Int. J. Comput. Meth. Appl. Mech. Engng.*, **118,** 393–412 (1994).
30. O. C. Zienkiewicz and R. L. Taylor, *The Finite Element Method*, Vol. I, McGraw-Hill, New York, 1989.

